Test Bench - Amplified Piezoelectric Actuator

Dehaeze Thomas
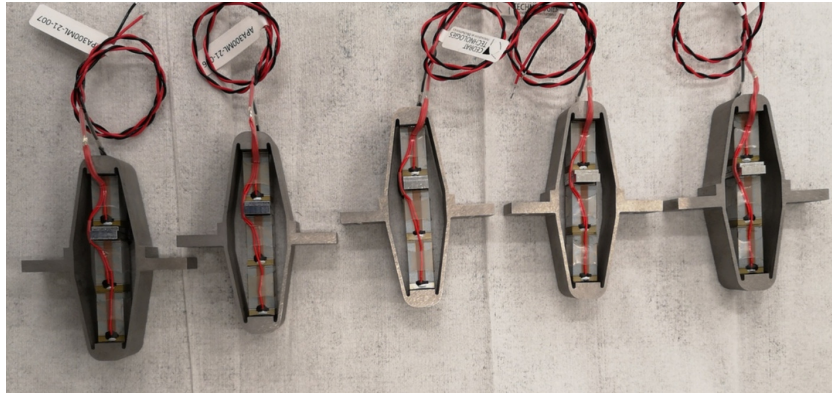
March 21, 2024

Contents

Figure 1: Picture of 5 out of the 7 received APA300ML

The first goal is to characterize the APA300ML in terms of:

- The, geometric features, electrical capacitance, stroke, hysteresis, spurious resonances. This is performed in Section 1.

- The dynamics from the generated DAC voltage (going to the voltage amplifiers and then applied on the actuator stacks) to the induced displacement, and to the measured voltage by the force sensor stack. Also the "actuator constant" and "sensor constant" are identified. This is done in Section 2.

- Compare the measurements with the Simscape models (2DoF, Super-Element) in order to tuned/-validate the models. This is explained in Section 3.

Table 1: Report sections and corresponding Matlab files

Sections	Matlab File
Section 1	`test_apa_1_basic_meas.m`
Section 2	`test_apa_2_.m`
Section 3	`test_apa_3_.m`

1 First Basic Measurements

Before using the measurement bench to characterize the APA300ML, first simple measurements are performed:

- Section 1.1: the geometric tolerances of the interface planes are checked

- Section 1.2: the capacitance of the piezoelectric stacks is measured

- Section 1.3: the stroke of each APA is measured

- Section 1.4: the "spurious" resonances of the APA are investigated

1.1 Geometrical Measurements

To measure the flatness of the two mechanical interfaces of the APA300ML, a small measurement bench is installed on top of a metrology granite with very good flatness.

As shown in Figure 1.1, the APA is fixed to a clamp while a measuring probe[1] is used to measure the height of 4 points on each of the APA300ML interfaces.

From the X-Y-Z coordinates of the measured 8 points, the flatness is estimated by best fitting[2] a plane through all the points.

The measured flatness, summarized in Table 1.1, are within the specifications.

Table 1.1: Estimated flatness of the APA300ML interfaces

	Flatness $[\mu m]$
APA 1	8.9
APA 2	3.1
APA 3	9.1
APA 4	3.0
APA 5	1.9
APA 6	7.1
APA 7	18.7

---

[1]Heidenhain MT25, specified accuracy of $0.5\,\mu m$
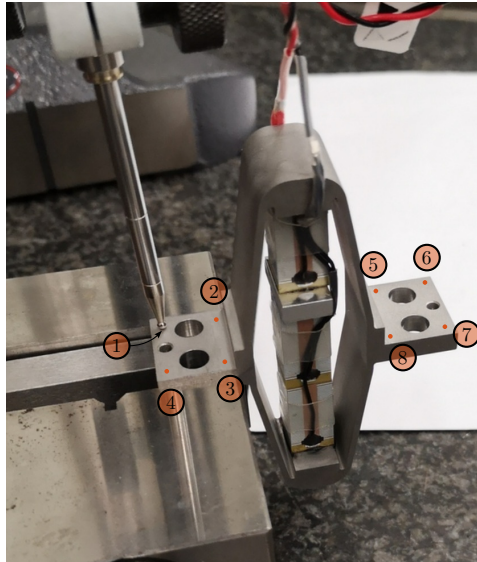[2]The Matlab `fminsearch` command is used to fit the plane

Figure 1.1: Measurement setup for flatness estimation of the two mechanical interfaces

1.2 Electrical Measurements

From the documentation of the APA300ML, the total capacitance of the three stacks should be between $18\,\mu F$ and $26\,\mu F$ with a nominal capacitance of $20\,\mu F$.

The capacitance of the piezoelectric stacks found in the APA300ML have been measured with the LCR meter[3] shown in Figure 1.2. The two stacks used as an actuator and the stack used as a force sensor are measured separately.
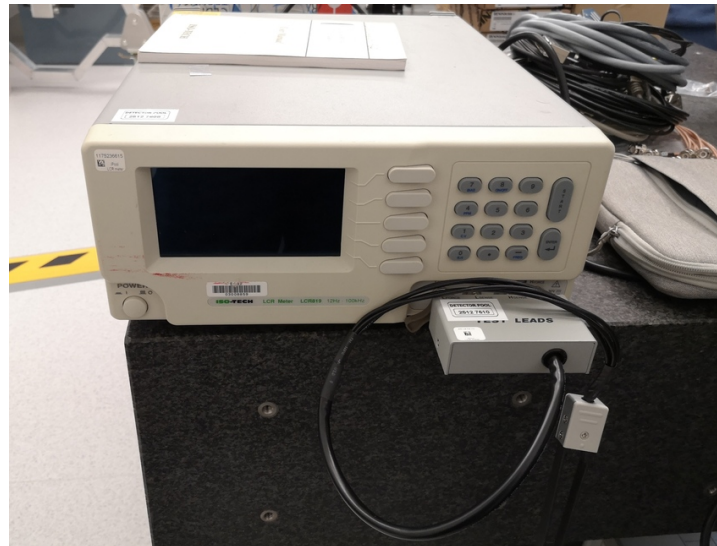

Figure 1.2: LCR Meter used for the measurements

The measured capacitance are summarized in Table 1.2 and the average capacitance of one stack is

---

[3]LCR-819 from Gwinstek, specified accuracy of 0.05%, measured frequency is set at $1\,kHz$

$\approx 5\mu F$. However, the measured capacitance of the stacks of "APA 3" is only half of the expected capacitance. This may indicate a manufacturing defect.

The measured capacitance is found to be lower than the specified one. This may be due to the fact that the manufacturer measures the capacitance with large signals ($-20\,V$ to $150\,V$) while it was here measured with small signals.

Table 1.2: Capacitance measured with the LCR meter. The excitation signal is a sinus at 1kHz

	Sensor Stack	Actuator Stacks
APA 1	5.10	10.03
APA 2	4.99	9.85
APA 3	1.72	5.18
APA 4	4.94	9.82
APA 5	4.90	9.66
APA 6	4.99	9.91
APA 7	4.85	9.85

1.3 Stroke Measurement

The goal is here to verify that the stroke of the APA300ML is as specified in the datasheet. To do so, one side of the APA is fixed to the granite, and a displacement probe[4] is located on the other side as shown in Figure 1.3.

Then, the voltage across the two actuator stacks is varied from $-20\,V$ to $150\,V$ using a DAC and a voltage amplifier. Note that the voltage is here slowly varied as the displacement probe has a very low measurement bandwidth (see Figure 1.3, left).

The measured APA displacement is shown as a function of the applied voltage in Figure 1.4, right.

Typical hysteresis curves for piezoelectric stack actuators can be observed. The measured stroke is approximately $250\,\mu m$ when using only two of the three stacks, which is enough for the current application. This is even above what is specified as the nominal stroke in the data-sheet ($304\,\mu m$, therefore $\approx 200\,\mu m$ if only two stacks are used).

It is clear from Figure 1.4 that "APA 3" has an issue compared to the other units. This confirms the abnormal electrical measurements made in Section 1.2. This unit was send sent back to Cedrat and a new one was shipped back. From now on, only the six APA that behave as expected will be used.

1.4 Spurious resonances - APA   @philipp

1.4.1 Introduction

From a Finite Element Model of the struts, it have been found that three main resonances are foreseen to be problematic for the control of the APA300ML (Figure 1.5):

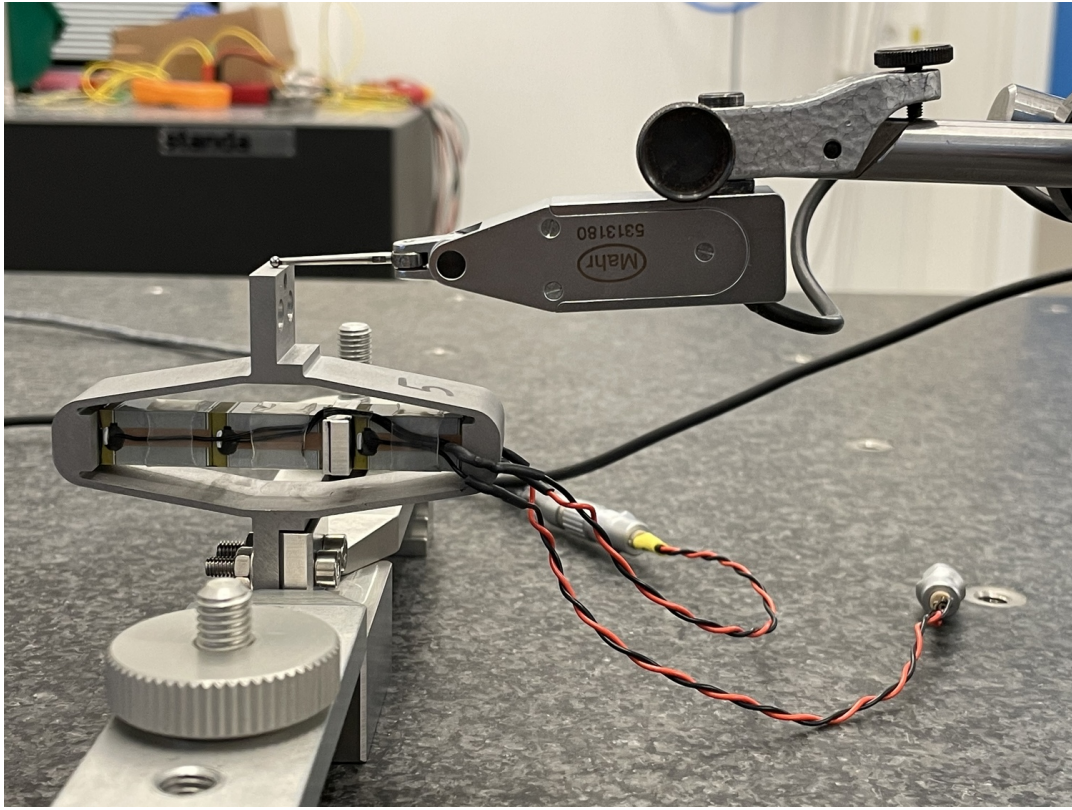[4]Millimar 1318 probe, specified linearity better than $1\,\mu m$

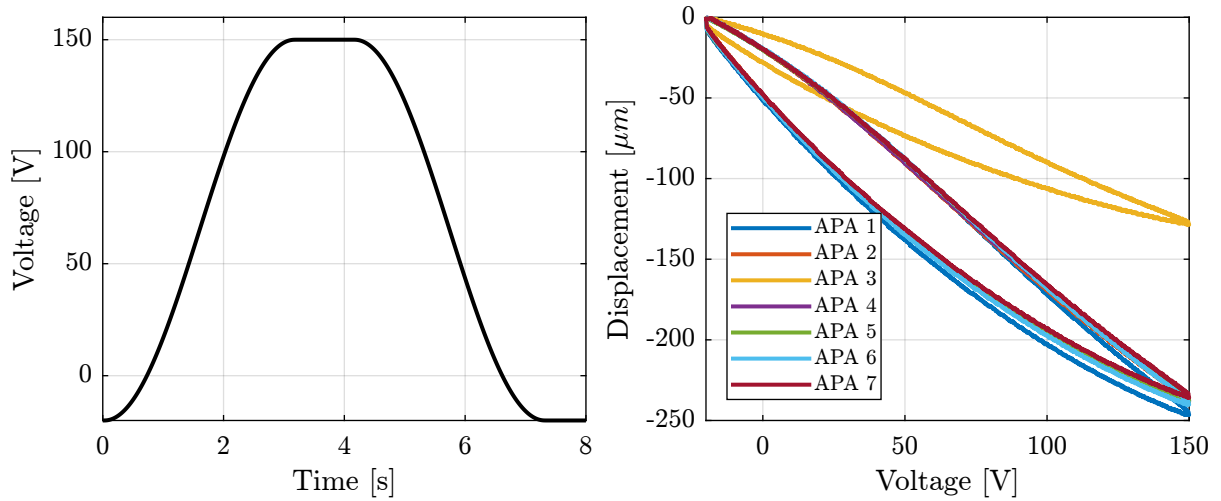**Figure 1.3:** Bench to measured the APA stroke

Figure 1.4: Generated voltage across the two piezoelectric stack actuators to estimate the stroke of the APA300ML (left). Measured displacement as a function of the applied voltage (right)

- Mode in X-bending at 189Hz

- Mode in Y-bending at 285Hz
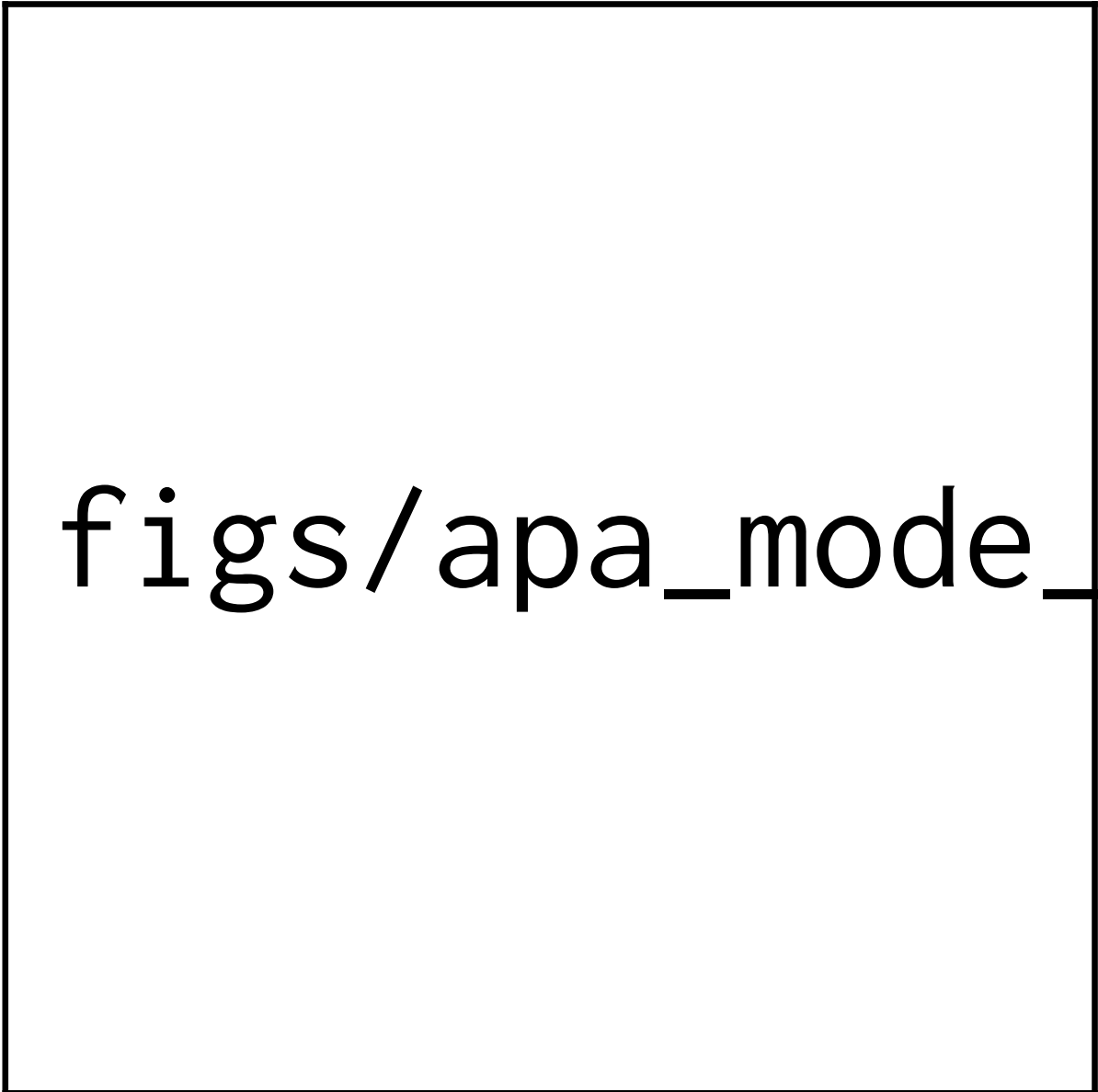
- Mode in Z-torsion at 400Hz

Figure 1.5: Spurious resonances. a) X-bending mode at 189Hz. b) Y-bending mode at 285Hz. c) Z-torsion mode at 400Hz

These modes are present when flexible joints are fixed to the ends of the APA300ML.

In this section, we try to find the resonance frequency of these modes when one end of the APA is fixed and the other is free.

In the section **??**, a similar measurement will be performed directly on the struts.

1.4.2 Measurement Setup

The measurement setup is shown in Figure 1.6. A Laser vibrometer is measuring the difference of motion between two points. The APA is excited with an instrumented hammer and the transfer function from the hammer to the measured rotation is computed.

> **Note**
>
> The instrumentation used are:
>
> - Laser Doppler Vibrometer Polytec OFV512
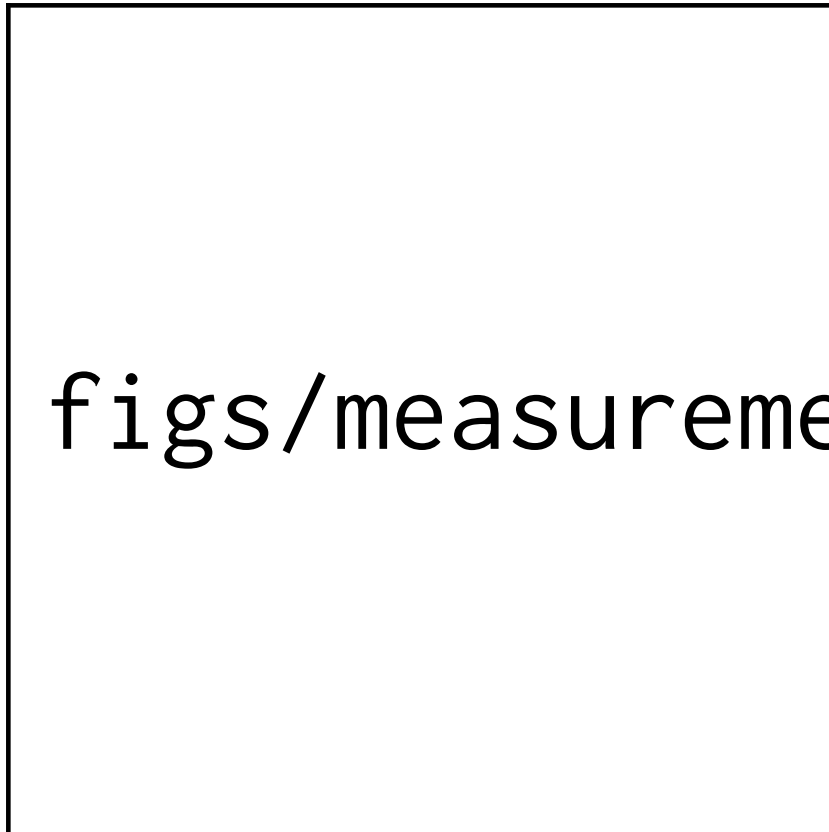>
> - Instrumented hammer

Figure 1.6: Measurement setup with a Laser Doppler Vibrometer and one instrumental hammer

1.4.3 X-Bending Mode

The vibrometer is setup to measure the X-bending motion is shown in Figure 1.7. The APA is excited with an instrumented hammer having a solid metallic tip. The impact point is on the back-side of the APA aligned with the top measurement point.

The data is loaded. The configuration (Sampling time and windows) for `tfestimate` is done: The transfer function from the input force to the output "rotation" (difference between the two measured distances). The result is shown in Figure 1.8.
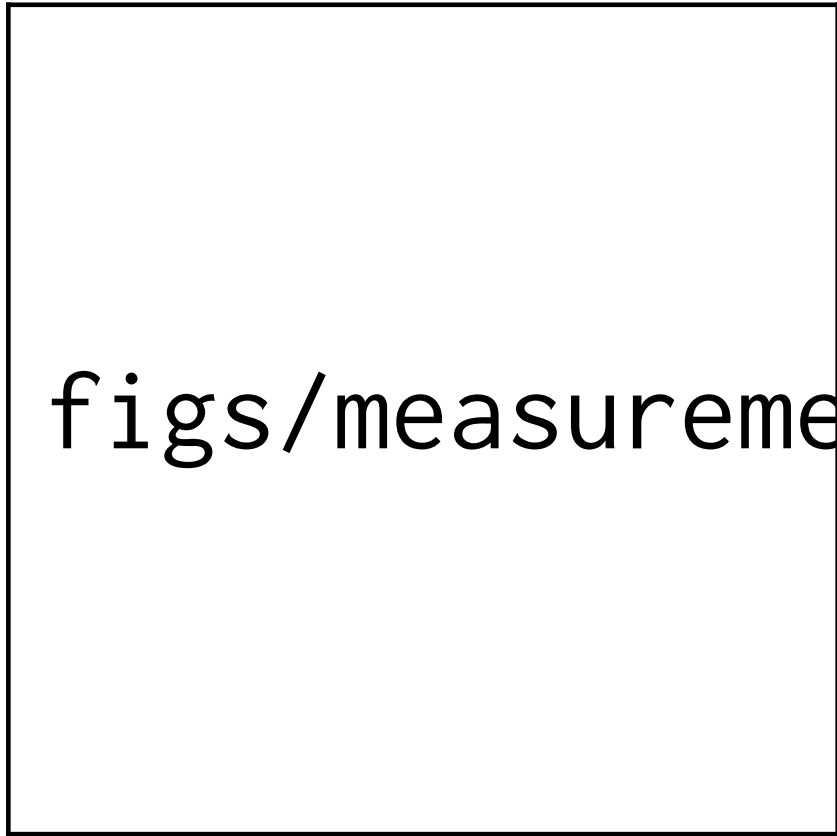
figs/measurement_setu

Figure 1.7: X-Bending measurement setup

The can clearly observe a nice peak at 280Hz, and then peaks at the odd "harmonics" (third "harmonic" at 840Hz, and fifth "harmonic" at 1400Hz).
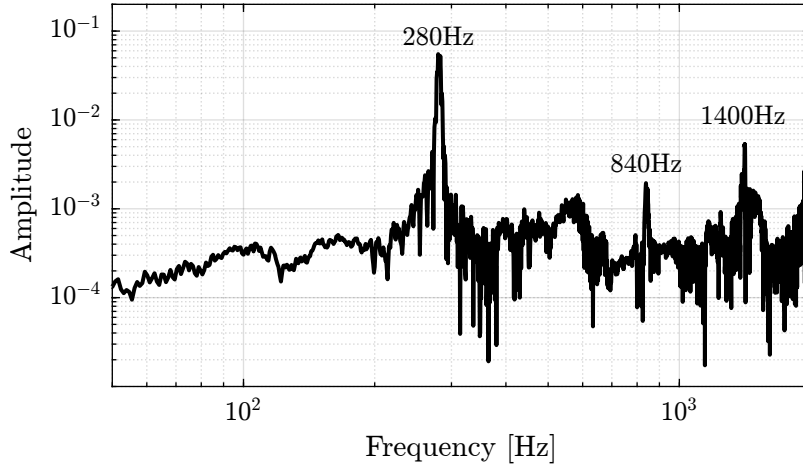

Figure 1.8: Obtained FRF for the X-bending

Then the APA is in the "free-free" condition, this bending mode is foreseen to be at 200Hz (Figure 1.5). We are here in the "fixed-free" condition. If we consider that we therefore double the stiffness associated with this mode, we should obtain a resonance a factor $\sqrt{2}$ higher than 200Hz which is indeed 280Hz. Not sure this reasoning is correct though.

1.4.4 Y-Bending Mode

The setup to measure the Y-bending is shown in Figure 1.9.

The impact point of the instrumented hammer is located on the back surface of the top interface (on the back of the 2 measurements points).

The data is loaded, and the transfer function from the force to the measured rotation is computed. The results are shown in Figure 1.10. The main resonance is at 412Hz, and we also see the third "harmonic" at 1220Hz.

We can apply the same reasoning as in the previous section and estimate the mode to be a factor $\sqrt{2}$ higher than the mode estimated in the "free-free" condition. We would obtain a mode at 403Hz which is very close to the one estimated here.

1.4.5 Z-Torsion Mode

Finally, we measure the Z-torsion resonance as shown in Figure 1.11.

The excitation is shown on the other side of the APA, on the side to excite the torsion motion.

The data is loaded, and the transfer function computed. The results are shown in Figure 1.12. We observe a first peak at 267Hz, which corresponds to the X-bending mode that was measured at 280Hz.
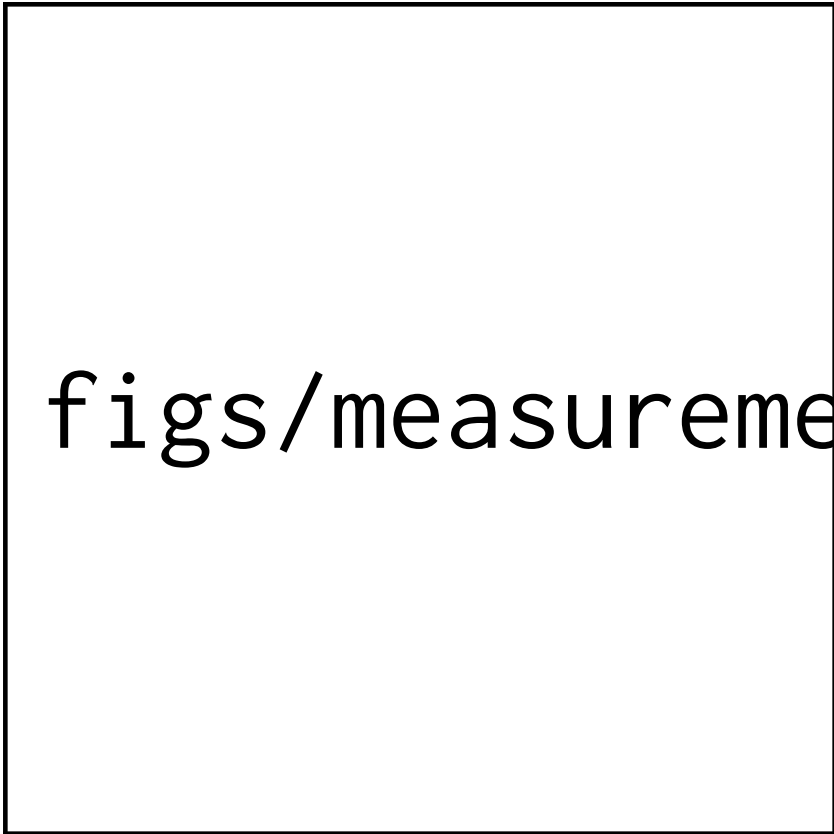
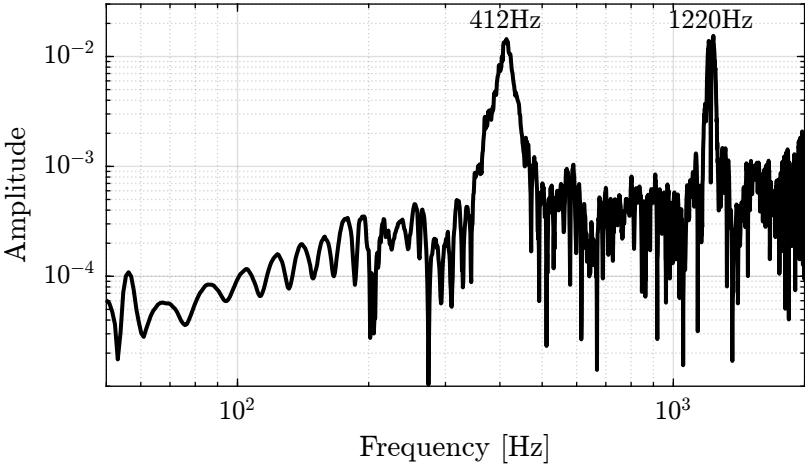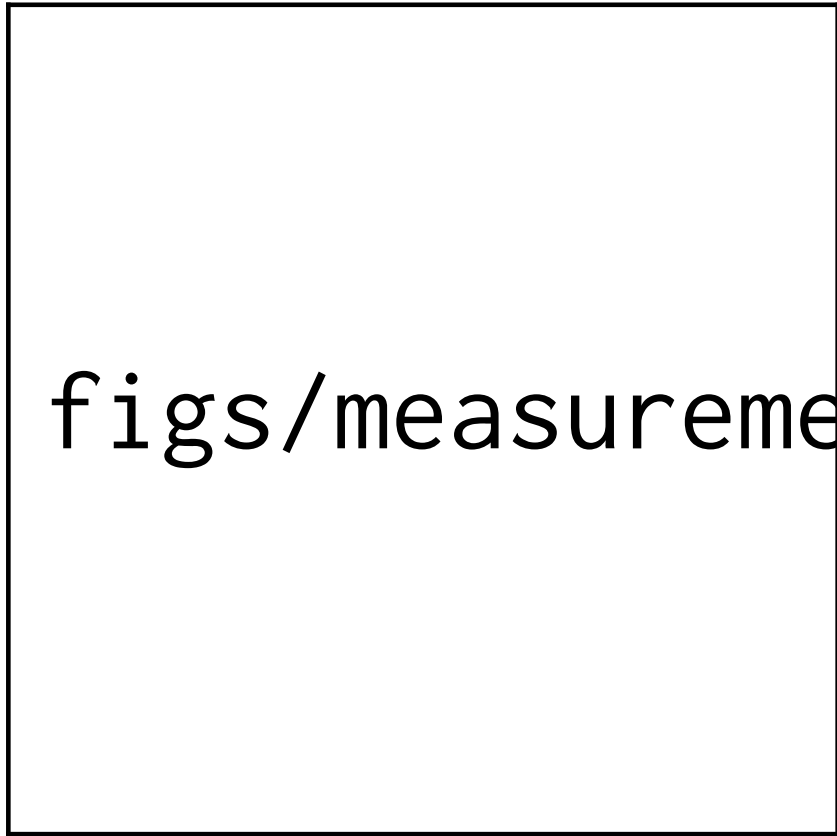**Figure 1.9:** Y-Bending measurement setup

Figure 1.10: Obtained FRF for the Y-bending

figs/measurement_setu

Figure 1.11: Z-Torsion measurement setup

And then a second peak at 415Hz, which corresponds to the X-bending mode that was measured at 412Hz. A third mode at 800Hz could correspond to this torsion mode.
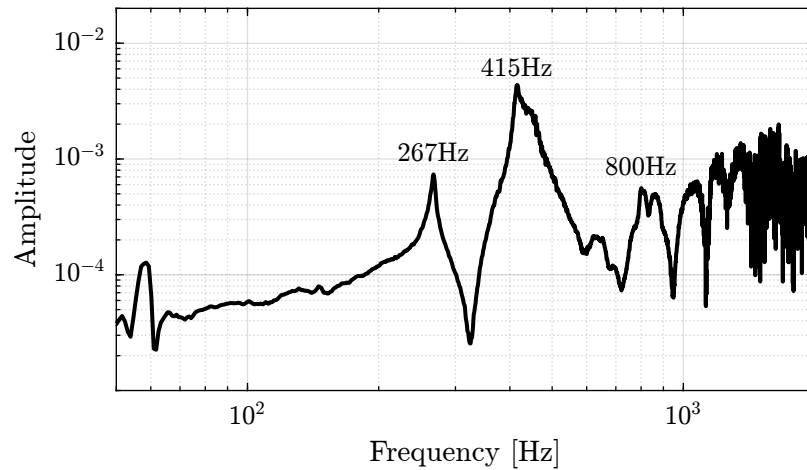

Figure 1.12: Obtained FRF for the Z-torsion

In order to verify that, the APA is excited on the top part such that the torsion mode should not be excited. The two FRF are compared in Figure 1.13. It is clear that the first two modes does not correspond to the torsional mode. Maybe the resonance at 800Hz, or even higher resonances. It is difficult to conclude here.
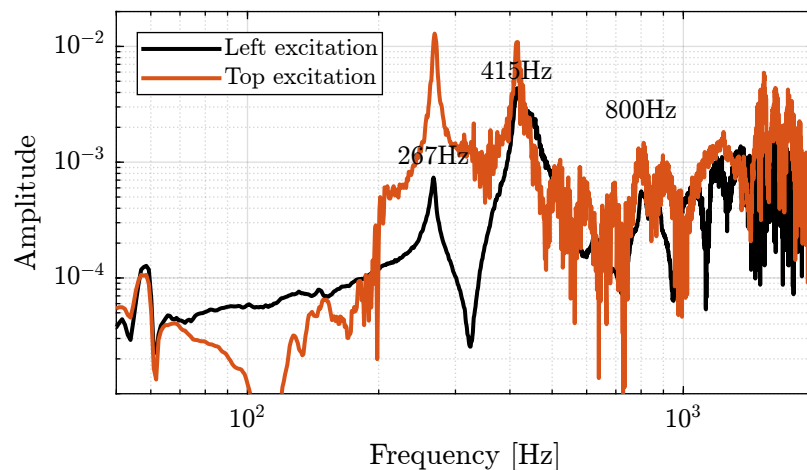

Figure 1.13: Obtained FRF for the Z-torsion

1.4.6 Compare

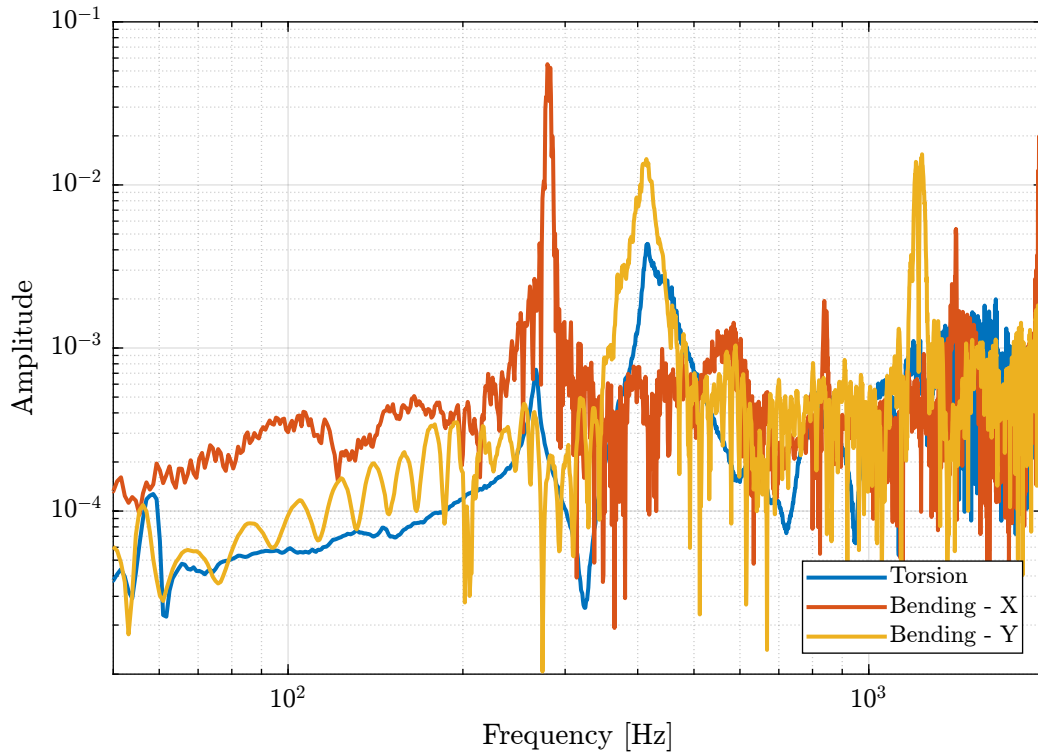The three measurements are shown in Figure 1.14.

Figure 1.14: Obtained FRF - Comparison

1.4.7 Conclusion

When two flexible joints are fixed at each ends of the APA, the APA is mostly in a free/free condition in terms of bending/torsion (the bending/torsional stiffness of the joints being very small).

In the current tests, the APA are in a fixed/free condition. Therefore, it is quite obvious that we measured higher resonance frequencies than what is foreseen for the struts. It is however quite interesting that there is a factor $\approx \sqrt{2}$ between the two (increased of the stiffness by a factor 2?).

Table 1.3: Measured frequency of the modes

Mode	FEM - Strut mode	Measured Frequency
X-Bending	189Hz	280Hz
Y-Bending	285Hz	410Hz
Z-Torsion	400Hz	800Hz?

2 Dynamical measurements - APA

After the basic measurements on the APA were performed in Section 1, a new test bench is used to better characterize the APA.

This test bench is shown in Figure 2.1 and consists of the APA300ML fixed on one end to the fixed granite, and on the other end to the 5kg granite vertically guided with an air bearing. An encoder is used to measure the relative motion between the two granites (i.e. the displacement of the APA).

The bench is schematically shown in Figure 2.2 and the signal used are summarized in Table 2.1.

Table 2.1: Variables used during the measurements

Variable	Description	Unit
u	Output DAC Voltage	V
V_a	Output Amplifier Voltage	V
V_s	Measured Stack Voltage (ADC)	V
d_e	Encoder Measurement	m

This bench will be used to:

- measure the dynamics of the APA (from V_a to d_e and d_a in Section **??**, and from V_a to V_s in section **??**)

- estimate the added damping using Integral Force Feedback (Section 2.5)

These measurements will also be used to tune the model of the APA in Section 3.

2.1 Hysteresis

As the payload is vertically guided without friction, the hysteresis of the APA can be estimated from the motion of the payload.

A quasi static sinusoidal excitation V_a with an offset of $65\,V$ (halfway between $-20\,V$ and $150\,V$), and an amplitude varying from $4\,V$ up to $80\,V$.

For each excitation amplitude, the vertical displacement d_e of the mass is measured and displayed as a function of the applied voltage..

The measured displacements as a function of the output voltages are shown in Figure 2.3. It is interesting to see that the hysteresis is increasing with the excitation amplitude.
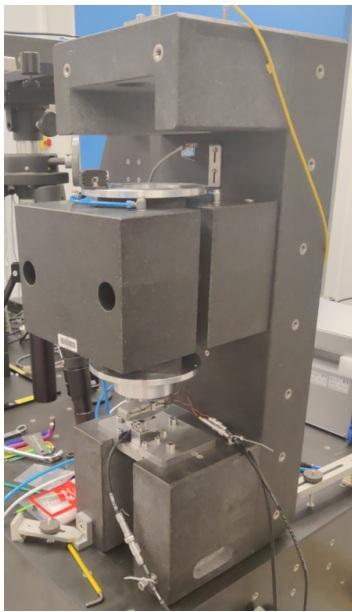
(a) Picture of the test bench
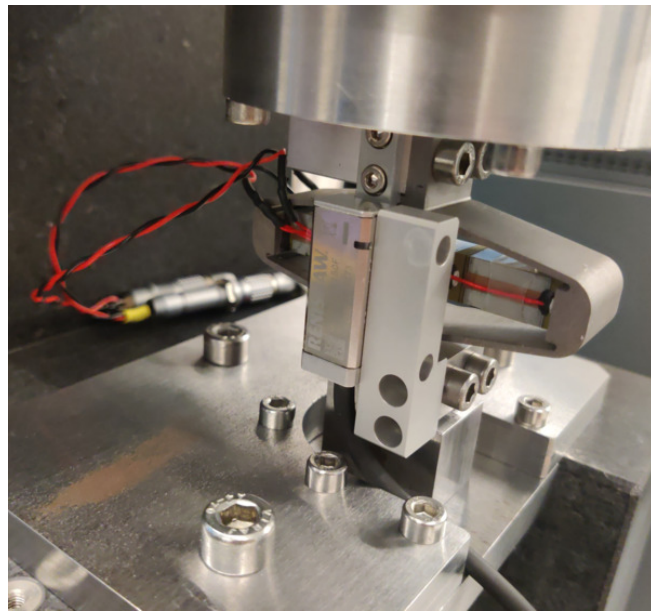
(b) Zoom on the APA with the encoder

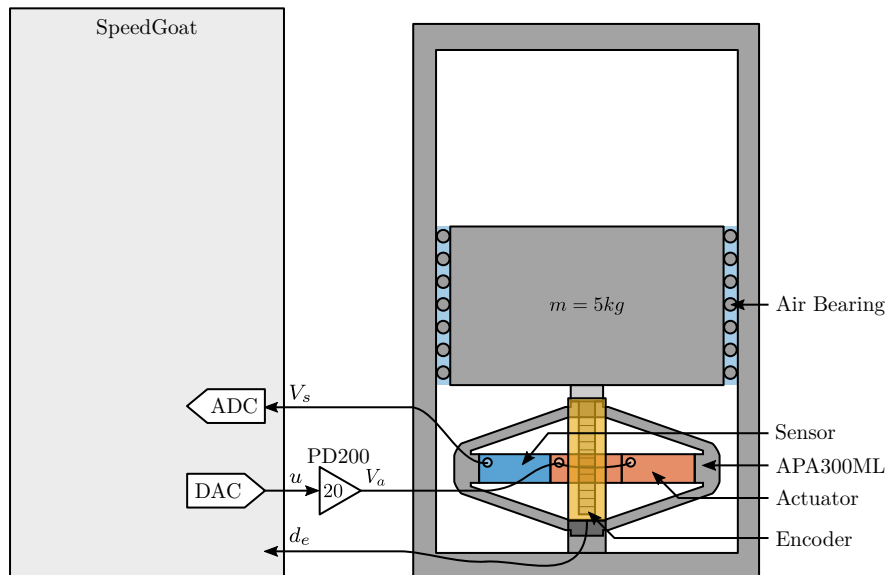**Figure 2.1:** Test bench used to characterize the APA300ML

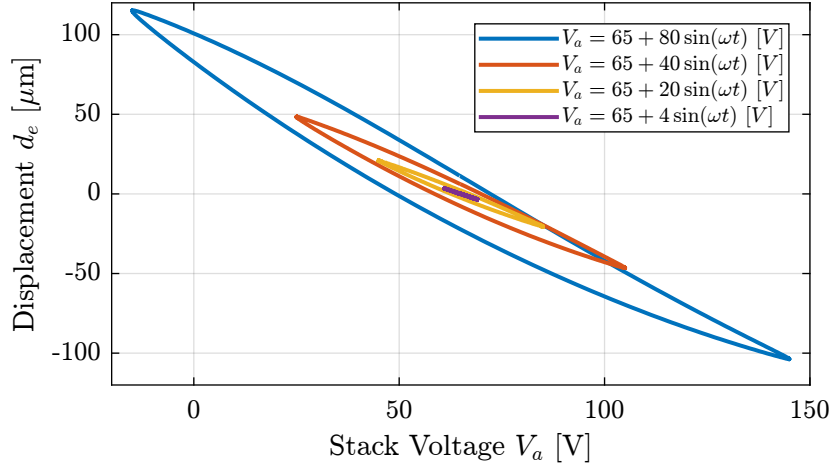**Figure 2.2:** Schematic of the Test Bench

Figure 2.3: Obtained hysteresis curves (displacement as a function of applied voltage) for multiple excitation amplitudes

2.2 Axial stiffness

In order to estimate the stiffness of the APA, a weight with known mass $m_a = 6.4\,\mathrm{kg}$ is added on top of the suspended granite and the deflection d_e is measured using the encoder.

The APA stiffness can then be estimated from equation (2.1).

$$k_{\mathrm{apa}} = \frac{m_a g}{\Delta d_e} \tag{2.1}$$

The measured displacement d_e as a function of time is shown in Figure 2.4. It can be seen that there are some drifts in the measured displacement (probably due to piezoelectric creep) and the that displacement does not come back to the initial position after the mass is removed (probably due to piezoelectric hysteresis). These two effects induce some uncertainties in the measured stiffness.

The stiffnesses are computed for all the APA from the two displacements d_1 and d_2 (see Figure 2.4) leading to two stiffness estimations k_1 and k_2. These estimated stiffnesses are summarized in Table 2.2 and are found to be close to the nominal stiffness $k = 1.8\,N/\mu m$ found in the APA300ML manual.

Table 2.2: Measured stiffnesses (in $N/\mu m$)

APA	k_1	k_2
1	1.68	1.9
2	1.69	1.9
4	1.7	1.91
5	1.7	1.93
6	1.7	1.92
8	1.73	1.98

The stiffness can also be computed using equation (2.2) by knowing the main vertical resonance frequency $\omega_z \approx 94\,\mathrm{Hz}$ (estimated by the dynamical measurements shown in section **??**) and the suspended
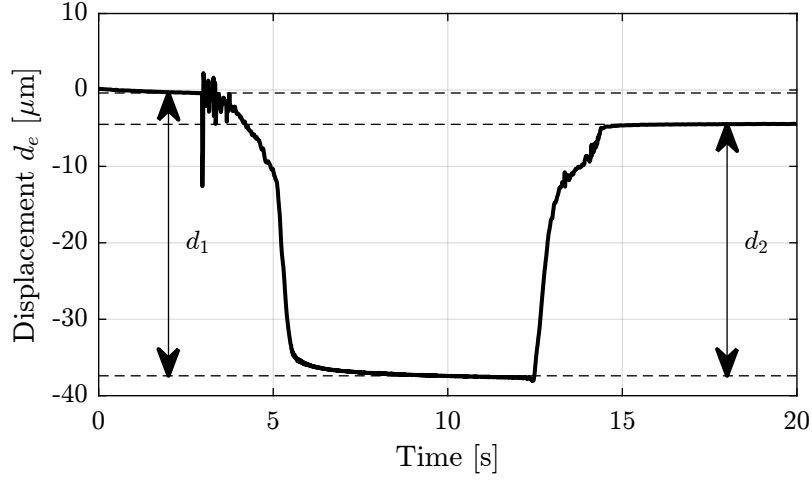
Figure 2.4: Measured displacement when adding the mass (at $t \approx 3\,s$) and removing the mass(at $t \approx 13\,s$)

mass $m_{\text{sus}} = 5.7\,\text{kg}$.

$$\omega_z = \sqrt{\frac{k}{m_{\text{sus}}}} \tag{2.2}$$

The obtain stiffness is $k \approx 2\,N/\mu m$ which is close to the values found in the documentation and by the "static deflection" method.

However, changes in the electrical impedance connected to the piezoelectric stacks impacts the mechanical compliance (or stiffness) of the piezoelectric stack [1, chap. 2].

To estimate this effect, the stiffness of the APA if measured using the "static deflection" method in two cases:

- k_{os}: piezoelectric stacks left unconnected (or connect to the high impedance ADC)

- k_{sc}: piezoelectric stacks short circuited (or connected to the voltage amplifier with small output impedance)

The open-circuit stiffness is estimated at $k_{\text{oc}} \approx 2.3\,N/\mu m$ and the closed-circuit stiffness $k_{\text{sc}} \approx 1.7\,N/\mu m$.

2.3 Dynamics

In this section, the dynamics of the system from the excitation voltage u to encoder measured displacement d_e and to the force sensor voltage V_s is identified.

The obtained transfer functions for the 6 APA between the excitation voltage u and the encoder displacement d_e are shown in Figure 2.5. The obtained transfer functions are close to a mass-spring-damper system. The following can be observed:

19

- A "stiffness line" indicating a static gain equal to $\approx -17\,\mu m/V$. The minus sign comes from the fact that an increase in voltage stretches the piezoelectric stack that then reduces the height of the APA

- A lightly damped resonance at $95\,\mathrm{Hz}$

- A "mass line" up to $\approx 800\,\mathrm{Hz}$, above which some resonances appear
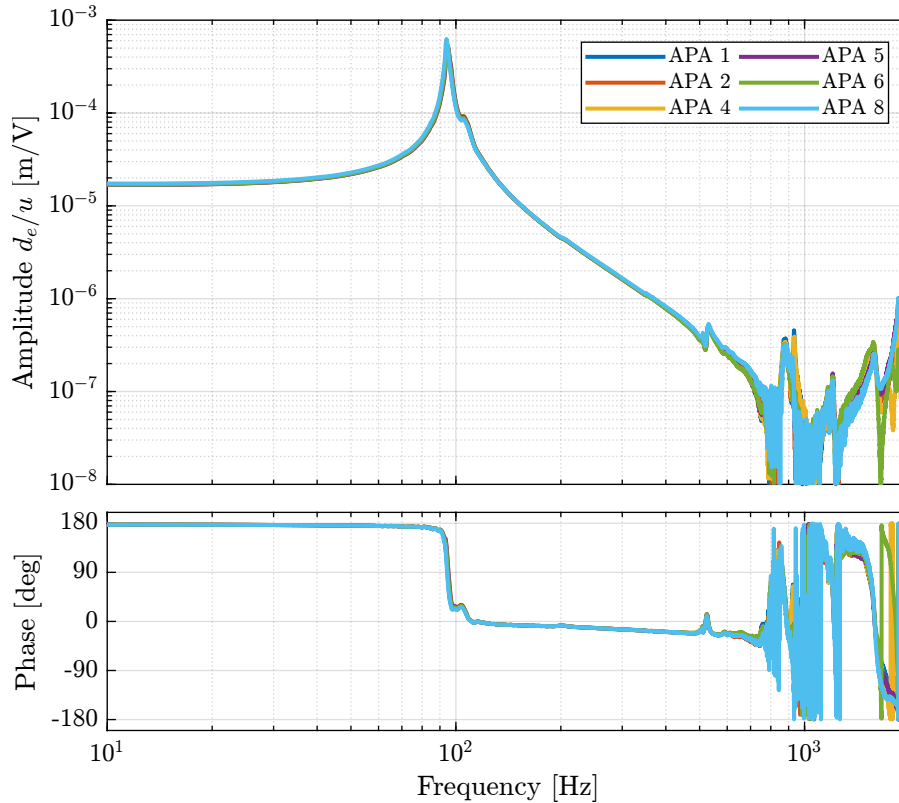

Figure 2.5: Estimated Frequency Response Function from generated voltage u to the encoder displacement d_e for the 6 APA300ML

The dynamics from u to the measured voltage across the sensor stack V_s is also identified and shown in Figure 2.6.

A lightly damped resonance is observed at $95\,\mathrm{Hz}$ and a lightly damped anti-resonance at $41\,\mathrm{Hz}$. No additional resonances is present up to at least $2\,\mathrm{kHz}$ indicating at Integral Force Feedback can be applied without stability issues from high frequency flexible modes.

As illustrated by the Root Locus, the poles of the closed-loop system converges to the zeros of the open-loop plant. Suppose that a controller with a very high gain is implemented such that the voltage V_s across the sensor stack is zero. In that case, because of the very high controller gain, no stress and strain is present on the sensor stack (and on the actuator stacks are well, as they are both in series). Such closed-loop system would therefore virtually corresponds to a system for which the piezoelectric stacks have been removed and just the mechanical shell is kept. From this analysis, the axial stiffness of the shell can be estimated to be $k_{\mathrm{shell}} = 5.7 \cdot (2\pi \cdot 41)^2 = 0.38\,N/\mu m$. Such reasoning can lead to very interesting insight into the system just from an open-loop identification.
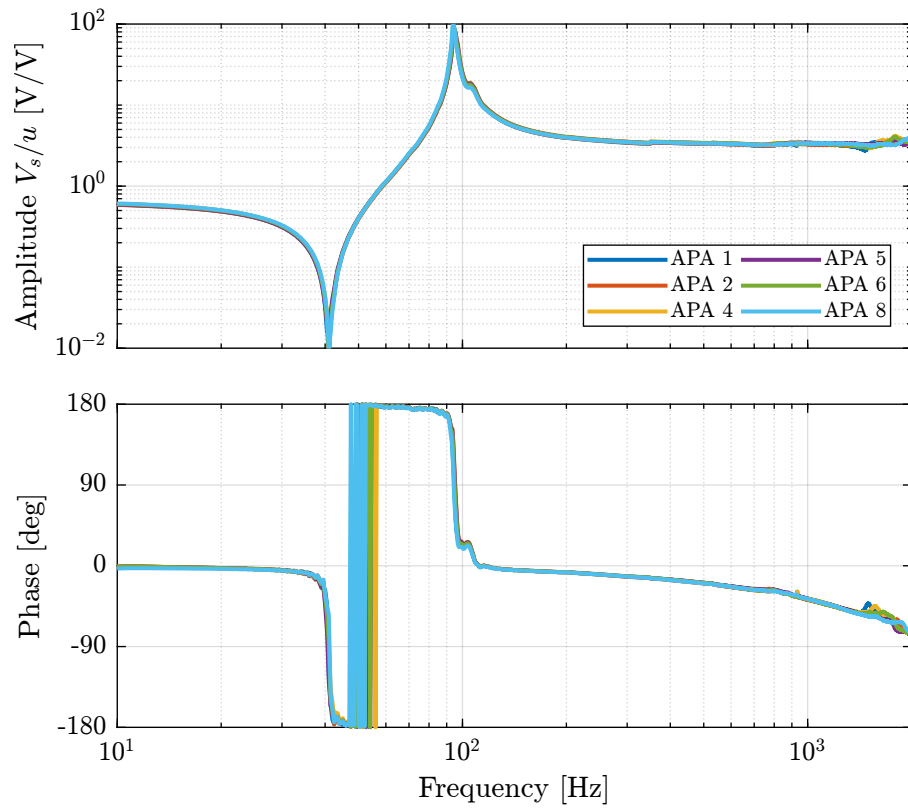
Figure 2.6: Estimated Frequency Response Function from generated voltage u to the sensor stack voltage V_s for the 6 APA300ML

All the identified dynamics of the six APA300ML (both when looking at the encoder in Figure 2.5 and at the force sensor in Figure 2.6) are almost identical, indicating good manufacturing repeatability for the piezoelectric stacks and the mechanical lever.

2.4 Effect of the resistor on the IFF Plant

A resistor $R \approx 80.6\,k\Omega$ is added in parallel with the sensor stack which has the effect to form a high pass filter with the capacitance of the stack.

As explain before, this is done for two reasons:

1. Limit the voltage offset due to the input bias current of the ADC

2. Limit the low frequency gain

The (low frequency) transfer function from u to V_s with and without this resistor have been measured and are compared in Figure 2.7. It is confirmed that the added resistor as the effect of adding an high pass filter with a cut-off frequency of $\approx 0.35\,\mathrm{Hz}$.
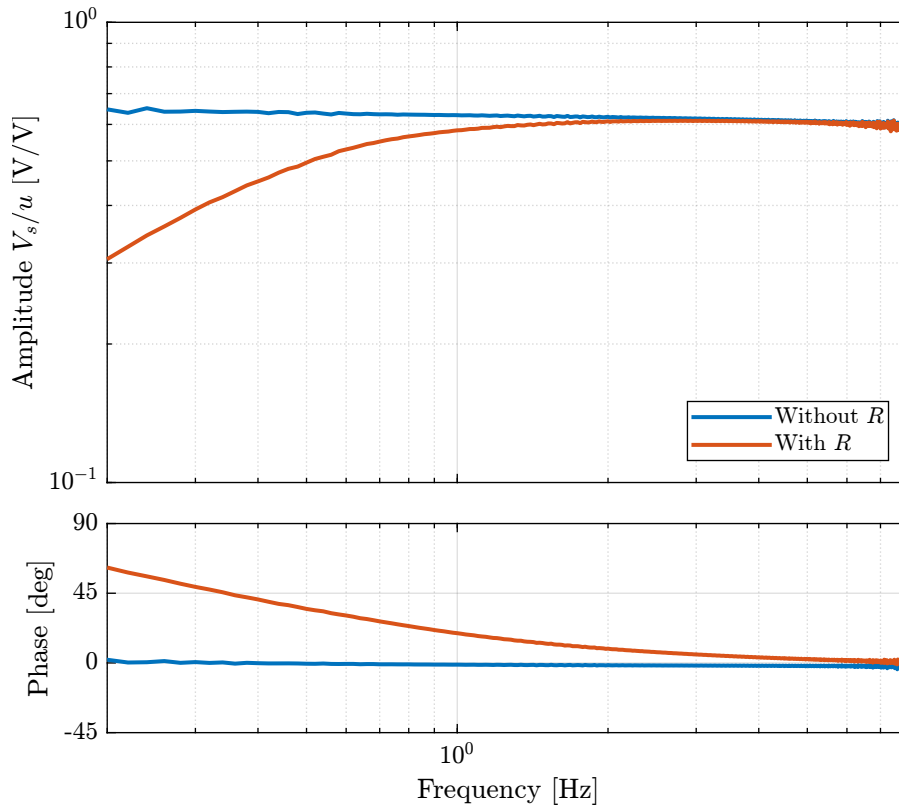

Figure 2.7: Transfer function from u to V_s with and without the resistor R in parallel with the piezo-electric stack used as the force sensor

2.5 Integral Force Feedback

This test bench can also be used to estimate the damping added by the implementation of an Integral Force Feedback strategy.

First, the transfer function (2.3) is manually tuned to match the identified dynamics from generated voltage u to the measured sensor stack voltage V_s in Section 2.3.

The obtained parameter values are $\omega_{\text{HPF}} = 0.4\,\text{Hz}$, $\omega_z = 42.7\,\text{Hz}$, $\xi_z = 0.4\,\%$, $\omega_p = 95.2\,\text{Hz}$, $\xi_p = 2\,\%$ and $g_0 = 0.64$.

$$G_{\text{IFF},m}(s) = g_0 \cdot \frac{1 + 2\xi_z \frac{s}{\omega_z} + \frac{s^2}{\omega_z^2}}{1 + 2\xi_p \frac{s}{\omega_p} + \frac{s^2}{\omega_p^2}} \cdot \frac{s}{\omega_{\text{HPF}} + s} \tag{2.3}$$

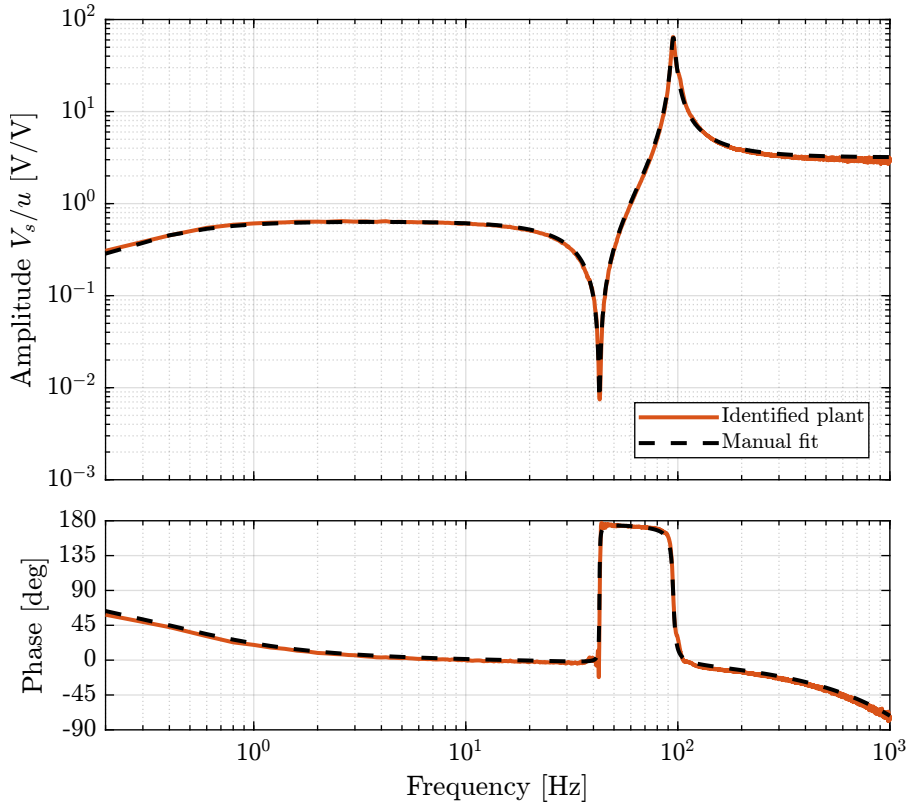The comparison between the identified plant and the manually tuned transfer function is done in Figure 2.8.

Figure 2.8: Identified IFF plant and manually tuned model of the plant (a time delay of $200\,\mu s$ is added to the model of the plant to better match the identified phase)

The implemented Integral Force Feedback Controller transfer function is shown in equation (2.4). It contains an high pass filter (cut-off frequency of $2\,\text{Hz}$) to limit the low frequency gain, a low pass filter to add integral action above $20\,\text{Hz}$, a second low pass filter to add robustness to high frequency resonances and a tunable gain g.

23

$$K_{\mathrm{IFF}}(s) = -10 \cdot g \cdot \frac{s}{s + 2\pi \cdot 2} \cdot \frac{1}{1 + 2\pi \cdot 20} \cdot \frac{1}{s + 2\pi \cdot 2000} \tag{2.4}$$

To estimate how the dynamics of the APA changes when the Integral Force Feedback controller is implemented, the test bench shown in Figure 2.9 is used. The transfer function from the "damped" plant input $u\prime$ to the encoder displacement d_e is identified for several IFF controller gains g.
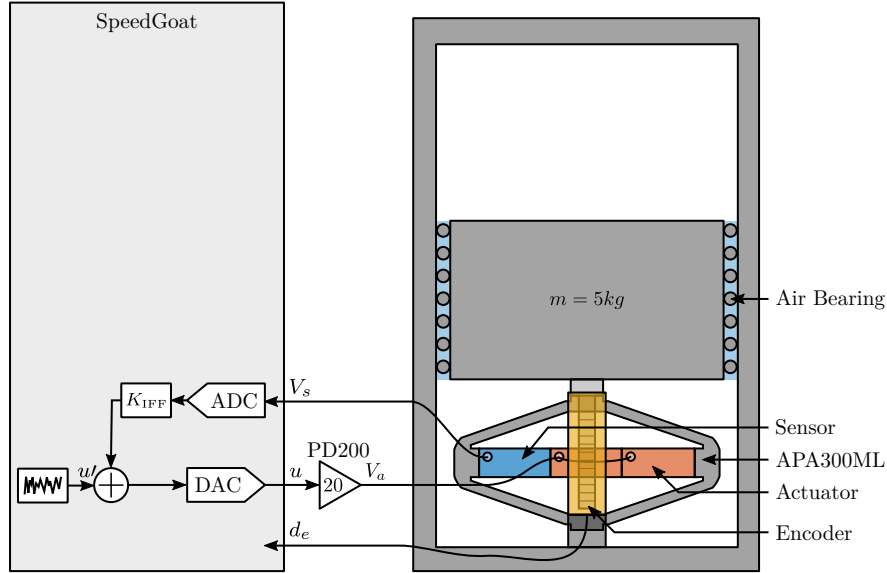

Figure 2.9: Figure caption

The identified dynamics are then fitted by second order transfer functions using the "Vector Fitting" toolbox [2]. The comparison between the identified damped dynamics and the fitted second order transfer functions is done in Figure 2.10 for different gains g. It is clear that large amount of damping is added when the gain is increased and that the frequency of the pole is shifted to lower frequencies.
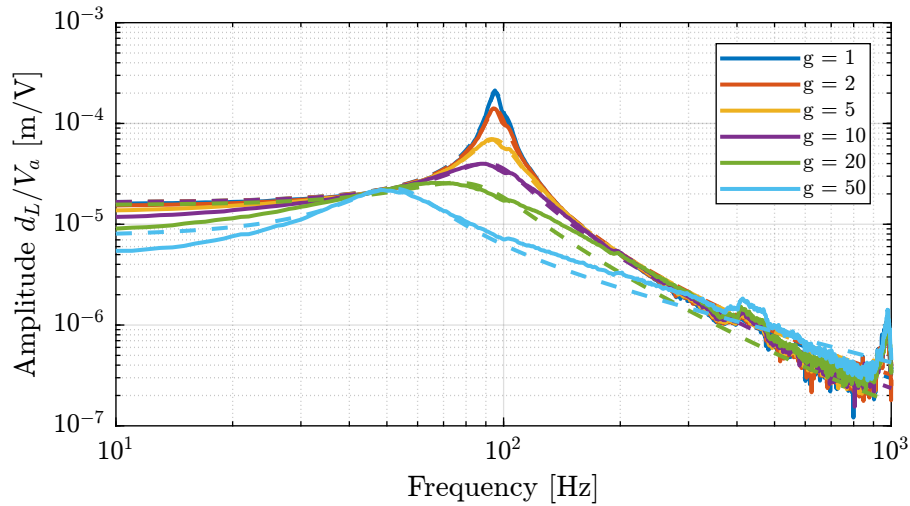

Figure 2.10: Identified dynamics (solid lines) and fitted transfer functions (dashed lines) from $u\prime$ to d_e for different IFF gains

24

The evolution of the pole in the complex plane as a function of the controller gain g (i.e. the "root locus") is computed:

- using the IFF plant model (2.3) and the implemented controller (2.4)

- from the fitted transfer functions of the damped plants experimentally identified for several controller gains

The two obtained root loci are compared in Figure 2.11 and are in good agreement considering that the damped plants were only fitted using a second order transfer function.
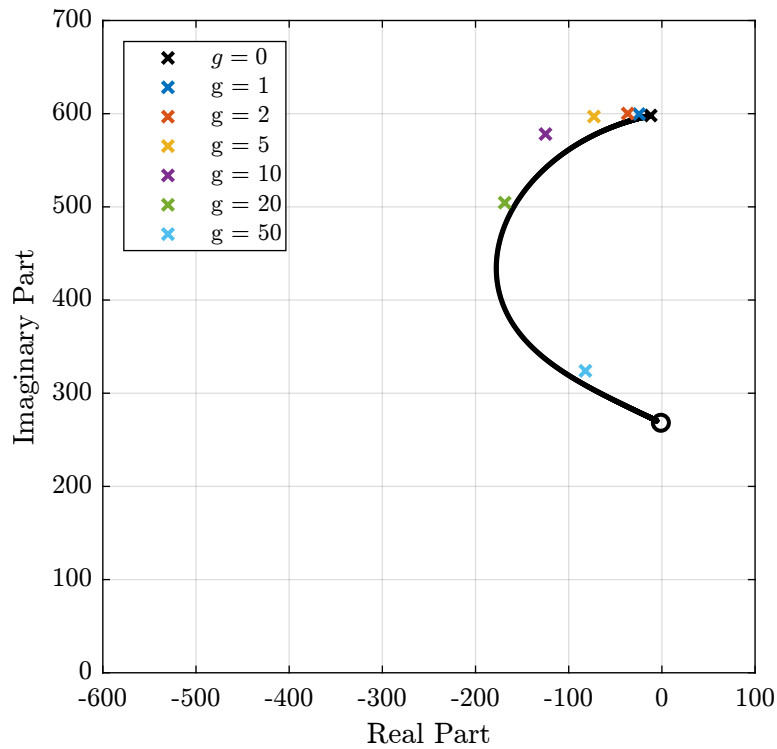

Figure 2.11: Root Locus of the APA300ML with Integral Force Feedback - Comparison between the computed root locus from the plant model (black line) and the root locus estimated from the damped plant pole identification (colorful crosses)

2.6 Conclusion

> **Important**
>
> So far, all the measured FRF are showing the dynamical behavior that was expected.

25

3 Test Bench APA300ML - Simscape Model

In this section, a simscape model (Figure 3.1) of the measurement bench is used to compare the model of the APA with the measured FRF.

After the transfer functions are extracted from the model (Section 3.1), the comparison of the obtained dynamics with the measured FRF will permit to:

1. Estimate the "actuator constant" and "sensor constant" (Section 3.2)

2. "Actuator constant": Gain from the applied voltage V_a to the generated Force F_a

3. "Sensor constant": Gain from the sensor stack strain δL to the generated voltage V_s

4. Tune the model of the APA to match the measured dynamics (Section 3.3)

3.1 First Identification

The APA is first initialized with default parameters: The transfer function from excitation voltage V_a (before the amplification of 20 due to the PD200 amplifier) to:

1. the sensor stack voltage V_s

2. the measured displacement by the encoder d_e

The obtain dynamics are shown in Figure 3.2 and 3.3. It can be seen that:

- the shape of these bode plots are very similar to the one measured in Section **??** expect from a change in gain and exact location of poles and zeros

- there is a sign error for the transfer function from V_a to V_s. This will be corrected by taking a negative "sensor gain".

- the low frequency zero of the transfer function from V_a to V_s is minimum phase as expected. The measured FRF are showing non-minimum phase zero, but it is most likely due to measurements artifacts.
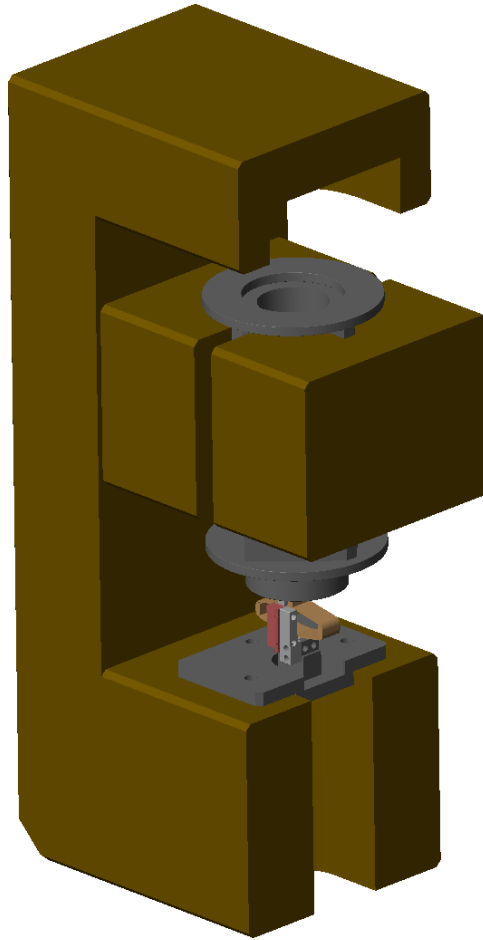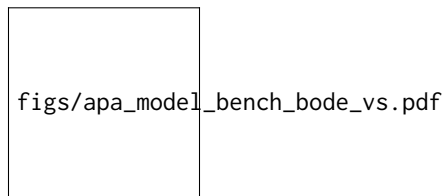
Figure 3.1: Screenshot of the Simscape model

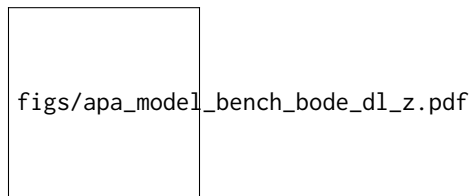

Figure 3.2: Bode plot of the transfer function from V_a to V_s

Figure 3.3: Bode plot of the transfer function from V_a to d_L and to z

3.2 Identify Sensor/Actuator constants and compare with measured FRF

3.2.1 How to identify these constants?

Piezoelectric Actuator Constant   Using the measurement test-bench, it is rather easy the determine the static gain between the applied voltage V_a to the induced displacement d.

$$d = g_{d/V_a} \cdot V_a \tag{3.1}$$

Using the Simscape model of the APA, it is possible to determine the static gain between the actuator force F_a to the induced displacement d:

$$d = g_{d/F_a} \cdot F_a \tag{3.2}$$

From the two gains, it is then easy to determine g_a:

$$\boxed{g_a = \frac{F_a}{V_a} = \frac{F_a}{d} \cdot \frac{d}{V_a} = \frac{g_{d/V_a}}{g_{d/F_a}}} \tag{3.3}$$

Piezoelectric Sensor Constant   Similarly, it is easy to determine the gain from the excitation voltage V_a to the voltage generated by the sensor stack V_s:

$$V_s = g_{V_s/V_a} V_a \tag{3.4}$$

Note here that there is an high pass filter formed by the piezoelectric capacitor and parallel resistor.

The gain can be computed from the dynamical identification and taking the gain at the wanted frequency (above the first resonance).

Using the simscape model, compute the gain at the same frequency from the actuator force F_a to the strain of the sensor stack dl:

$$dl = g_{dl/F_a} F_a \tag{3.5}$$

Then, the "sensor" constant is:

$$\boxed{g_s = \frac{V_s}{dl} = \frac{V_s}{V_a} \cdot \frac{V_a}{F_a} \cdot \frac{F_a}{dl} = \frac{g_{V_s/V_a}}{g_a \cdot g_{dl/F_a}}} \tag{3.6}$$

3.2.2 Identification Data

Let's load the measured FRF from the DAC voltage to the measured encoder and to the sensor stack voltage.

3.2.3 2DoF APA

2DoF APA   Let's initialize the APA as a 2DoF model with unity sensor and actuator gains.

Identification without actuator or sensor constants   The transfer function from V_a to V_s, d_e and d_a is identified.

Actuator Constant   Then, the actuator constant can be computed as shown in Eq. (3.3) by dividing the measured DC gain of the transfer function from V_a to d_e by the estimated DC gain of the transfer function from V_a (in truth the actuator force called F_a) to d_e using the Simscape model.

```
―――――――――――――――――――――――――――――――――――― Results ――――――――――――――――――――――――――――――――――――
ga = -32.2 [N/V]
```

Sensor Constant   Similarly, the sensor constant can be estimated using Eq. (3.6).

```
―――――――――――――――――――――――――――――――――――― Results ――――――――――――――――――――――――――――――――――――
gs = 0.088 [V/m]
```

Comparison   Let's now initialize the APA with identified sensor and actuator constant: And identify the dynamics with included constants. The transfer functions from V_a to d_e are compared in Figure 3.4 and the one from V_a to V_s are compared in Figure 3.5.
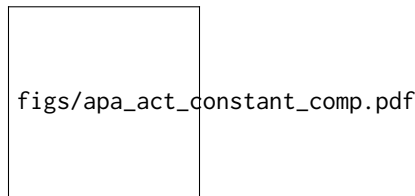

figs/apa_act_constant_comp.pdf

Figure 3.4: Comparison of the experimental data and Simscape model (V_a to d_e)
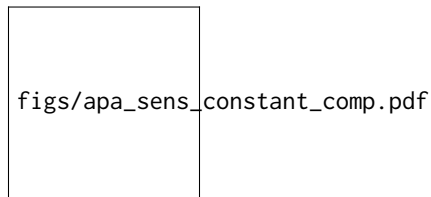

figs/apa_sens_constant_comp.pdf

Figure 3.5: Comparison of the experimental data and Simscape model (V_a to V_s)

> **Important**
>
> The "actuator constant" and "sensor constant" can indeed be identified using this test bench. After identifying these constants, the 2DoF model shows good agreement with the measured dynamics.

figs/apa_comp_model_frf.pdf

3.2.4 Flexible APA

In this section, the sensor and actuator "constants" are also estimated for the flexible model of the APA.

Flexible APA   The Simscape APA model is initialized as a flexible one with unity "constants".

Identification without actuator or sensor constants   The dynamics from V_a to V_s, d_e and d_a is identified.

Actuator Constant   Then, the actuator constant can be computed as shown in Eq. (3.3):

```
────────────────────────────────── Results ──────────────────────────────────
ga = 23.5 [N/V]
```

```
────────────────────────────────── Results ──────────────────────────────────
gs = -4839841.756 [V/m]
```

Sensor Constant

Comparison   Let's now initialize the flexible APA with identified sensor and actuator constant: And identify the dynamics with included constants. The obtained dynamics is compared with the measured one in Figures 3.6 and 3.7.

figs/apa_act_constant_comp_flex.pdf

Figure 3.6: Comparison of the experimental data and Simscape model (u to $d\mathcal{L}_m$)

> **Important**
>
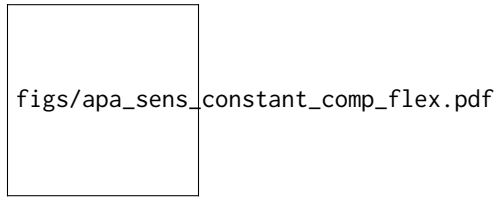> The flexible model is a bit "soft" as compared with the experimental results.

Figure 3.7: Comparison of the experimental data and Simscape model (u to τ_m)

3.3 Optimize 2-DoF model to fit the experimental Data

The parameters of the 2DoF model presented in Section **??** are now optimize such that the model best matches the measured FRF.

After optimization, the following parameters are used: The dynamics is identified using the Simscape model and compared with the measured FRF in Figure 3.8.
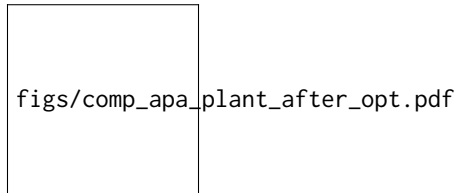

Figure 3.8: Comparison of the measured FRF and the optimized model

> **Important**
>
> The tuned 2DoF is very well representing the (axial) dynamics of the APA.

4 Conclusion

Bibliography

[1] M. Reza and F. Andrew, *Piezoelectric Transducers for Vibration Control and Damping.* London: Springer, 2006 (cit. on p. 19).

[2] A. Gustavsen B.; Semlyen, "Rational approximation of frequency domain responses by vector fitting," *IEEE Transactions on Power Delivery*, vol. 14, 3 Jul. 1999 (cit. on p. 24).